

## Supporting information

### Assemblies of Poly(N-Vinyl-2-Pyrrolidone)-Based Double Hydrophilic Block Copolymers Triggered by Lanthanide Ions: Characterization and Evaluation of their Properties as MRI Contrast Agent.

Marjorie Yon,<sup>a</sup> Laure Gibot,<sup>a</sup> Stéphane Gineste,<sup>a</sup> Pascale Laborie,<sup>b</sup> Christian Bijani,<sup>c</sup> Christophe Mingotaud,<sup>a</sup> Olivier Coutelier,<sup>a</sup> Franck Desmoulin,<sup>d,e</sup> Carine Pestourie,<sup>e</sup> Mathias Destarac,<sup>a</sup> Diana Ciuculescu-Pradines\*<sup>a</sup> and Jean-Daniel Marty\*<sup>a</sup>

#### Summary:

##### 1. Polymer characterization

- 1.1. <sup>1</sup>H NMR spectrum of poly(methyl acrylate) (PMA-XA<sub>1</sub>)
- 1.2. <sup>1</sup>H NMR spectrum of poly(methyl acrylate)-*block*-poly(N-vinyl-2-pyrrolidone) copolymer (PMA<sub>32</sub>-*b*-PVP<sub>59</sub>)
- 1.3. <sup>1</sup>H NMR spectrum of poly(acrylic acid)-*block*-poly(N-vinyl-2-pyrrolidone) copolymer (PAA<sub>32</sub>-*b*-PVP<sub>59</sub>)

##### 2. Characterization of HPICs

- 2.1. Dynamic Light Scattering and Zeta potential measurements
- 2.2. Transmission electron microscopy (TEM) and high-angle annular dark-field scanning transmission electron microscopy (HAADF-STEM) experiments
- 2.3. Photophysical Experiments
- 2.4. ATR-FTIR Experiments
- 2.5. <sup>1</sup>H NMR experiments-Y<sup>3+</sup>-titration
- 2.6. Random vs. block copolymer for the formation of HPICs

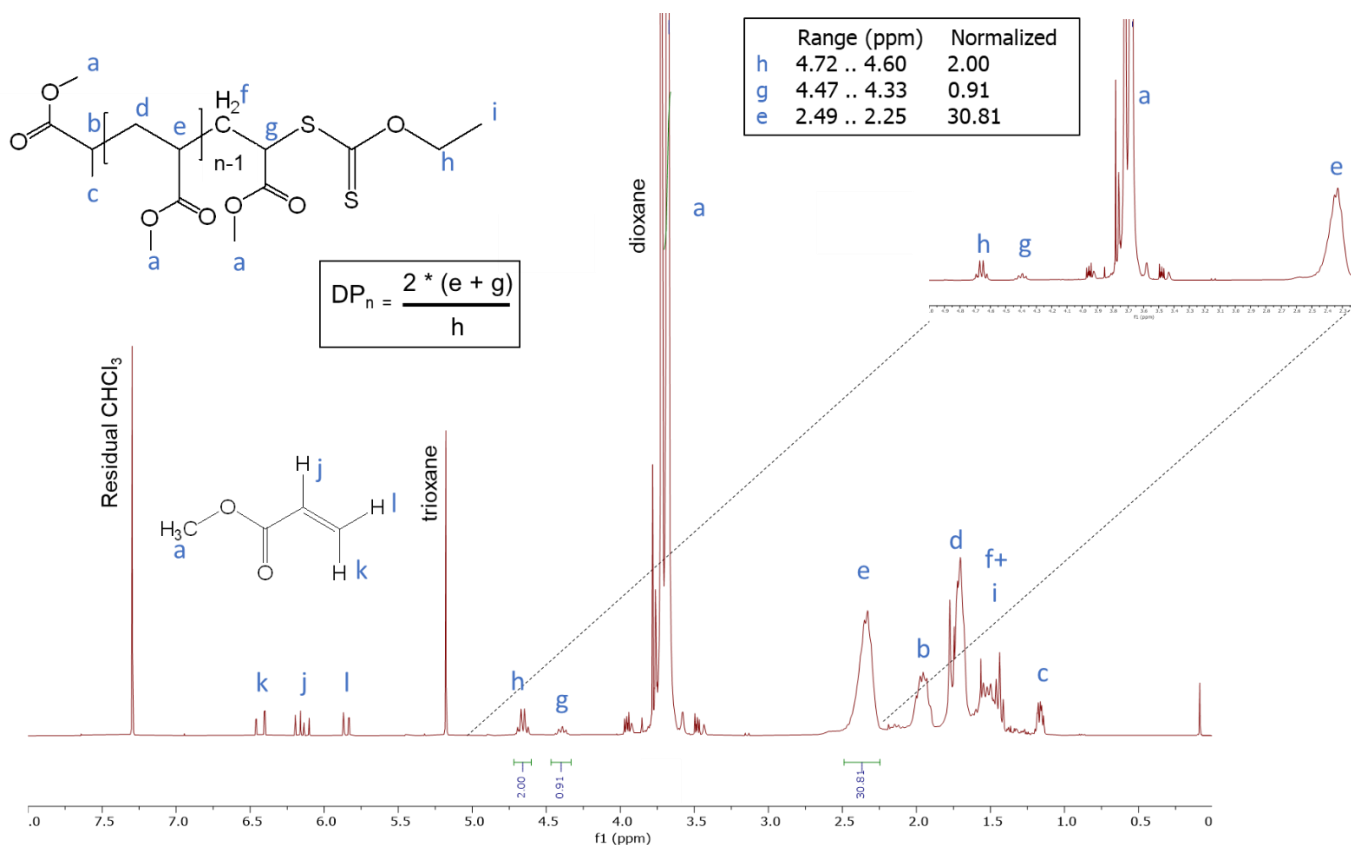
##### 3. Colloidal stability of HPICs and properties in biological medium

- 3.1. Stability in the presence of different NaCl concentrations
- 3.2. Influence of pH
- 3.3. Stability as a function of the dilution factor
- 3.4. Stability in complete cell culture medium

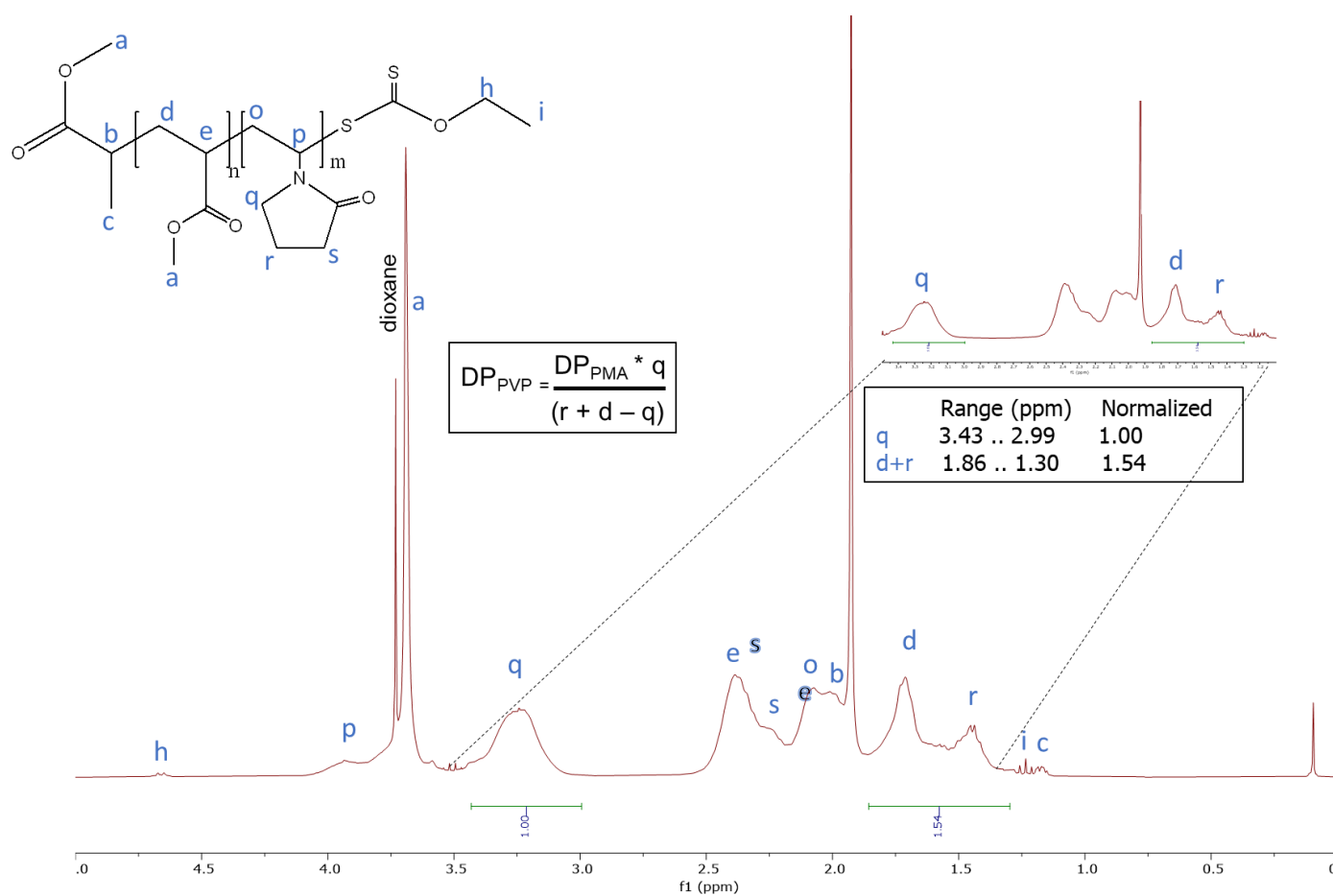
##### 4. Relaxivity measurements

##### 5. References

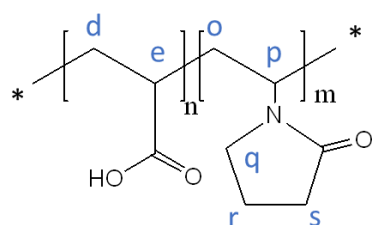
## 1. Polymer characterization

1.1.  $^1\text{H}$  NMR spectrum of poly(methyl acrylate) (PMA- $\text{XA}_1$ )

**Figure S1.**  $^1\text{H}$  NMR spectrum ( $\text{CDCl}_3$ ) of poly(methyl acrylate) homopolymer ( $\text{PMA}_{32}\text{-XA}_1$ ). The number-average degree of polymerization ( $DP_n$ ) was evaluated from the integration of the signals noted as e (1H,  $-\text{CH}-\text{COOMe}$  – 2.33 ppm) relative to the one of h (2H,  $-\text{CH}_2-\text{O}-\text{CS}$  – 4.66 ppm arbitrary fixed at 2), and the signal noted as g (1H,  $-\text{CH}_2-\text{CH}(\text{CO}_2\text{CH}_3)-\text{S}(\text{C}=\text{S})-\text{OCH}_2\text{CH}_3$  – 4.4 ppm) must be taken into account in the calculation of the DP as following :  $DP = \frac{2 * (e+g)}{h}$ .  $DP_n$  was estimated around 32.

1.2.  $^1\text{H}$  NMR spectrum of poly(methyl acrylate)-*block*-poly(N-vinyl-2-pyrrolidone) copolymer ( $\text{PMA}_{32}$ -*b*- $\text{PVP}_{59}$ )

**Figure S2.**  $^1\text{H}$  NMR spectrum ( $\text{CDCl}_3$ ) of poly(methyl acrylate)-*block*-poly(N-vinyl-2-pyrrolidone) copolymer ( $\text{PMA}_{32}$ -*b*- $\text{PVP}_{59}$ ). Degree of polymerization of N-VP ( $DP = 59$ ) can be evaluated by directly comparing the ratio of the integrals of signals of PVP (q signal) to the one of PVP plus PMA (r and d signals) assuming a degree of polymerization of PMA block of 32. The following equation was used:  $DP_{\text{PVP}} = \frac{DP(\text{PMA}) * q}{(r+d-q)}$

1.3.  $^1\text{H}$  NMR spectrum of poly(acrylic acid)-*block*-poly(N-vinyl-2-pyrrolidone) copolymer (PAA<sub>32</sub>-*b*-PVP<sub>59</sub>)

	Range (ppm)	Normalized
q	3.43 .. 2.99	1.00
u	2.58 .. 1.29	3.91

$$DP_{\text{PVP}} = \frac{3 * DP_{\text{PMA}}}{2 * (u - 3q)}$$

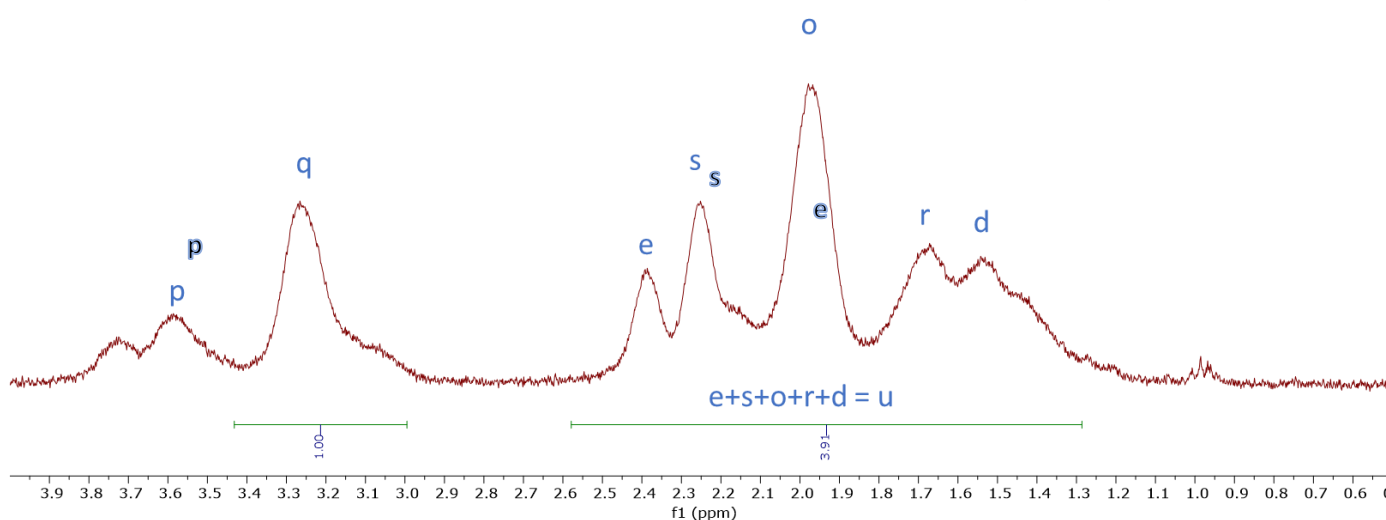


**Figure S3.**  $^1\text{H}$  NMR spectrum ( $\text{D}_2\text{O}$ ) of the poly(acrylic acid)-*block*-poly(N-vinyl-2-pyrrolidone) copolymer (PAA<sub>32</sub>-*b*-PVP<sub>59</sub>). Integrated signals enabled the calculation of the ratio between AA and NVP units.  $DP_n$  of PAA was considered equal to the  $DP_n$  of PMA as determined in the Fig. S1. Here the ratio between the two types of units of the copolymer was calculated considering a single integral for the protons ranging from 1.2 to 2.5 ppm which corresponds to  $3n\text{H}$  from the AA units and  $6m\text{H}$  from the NVP units normalized to the integral of the q ( $2n\text{H}$ ) protons of the NVP units. This strategy for the integration of the signals was chosen in order to minimize errors, because in the 1.2 to 2.5 ppm region the signals coming from the PVP and PAA overlap.

## 2. Characterization of HPICs

### 2.1. Dynamic Light Scattering and Zeta potential measurements

#### *Mono-angle dynamic light scattering*

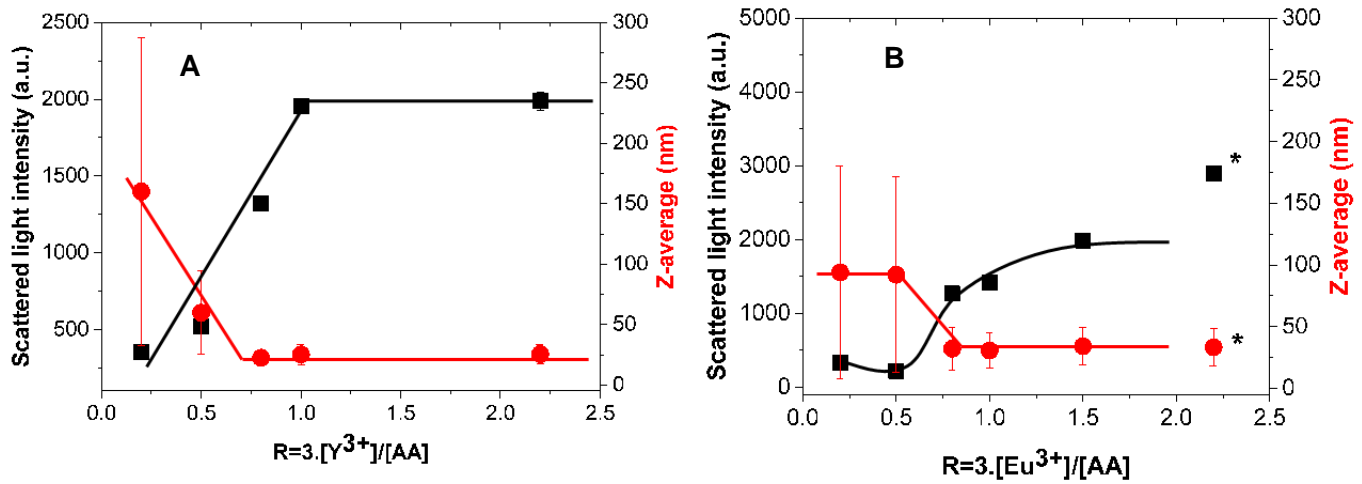


**Figure S4** A)  $Y^{3+}/PAA_{32}-b-PVP_{59}$  and B)  $Eu^{3+}/PAA_{32}-b-PVP_{59}$  HPICs versus the ratio  $R$ . The lines are just guide for the eyes. In the case of Eu based HPICs, at the highest ratio ( $R=2.2$ ) the formation of hydroxide species is suspected as evidenced by ATR-FTIR experiments, so corresponding values does not belong solely to HPICs formation.

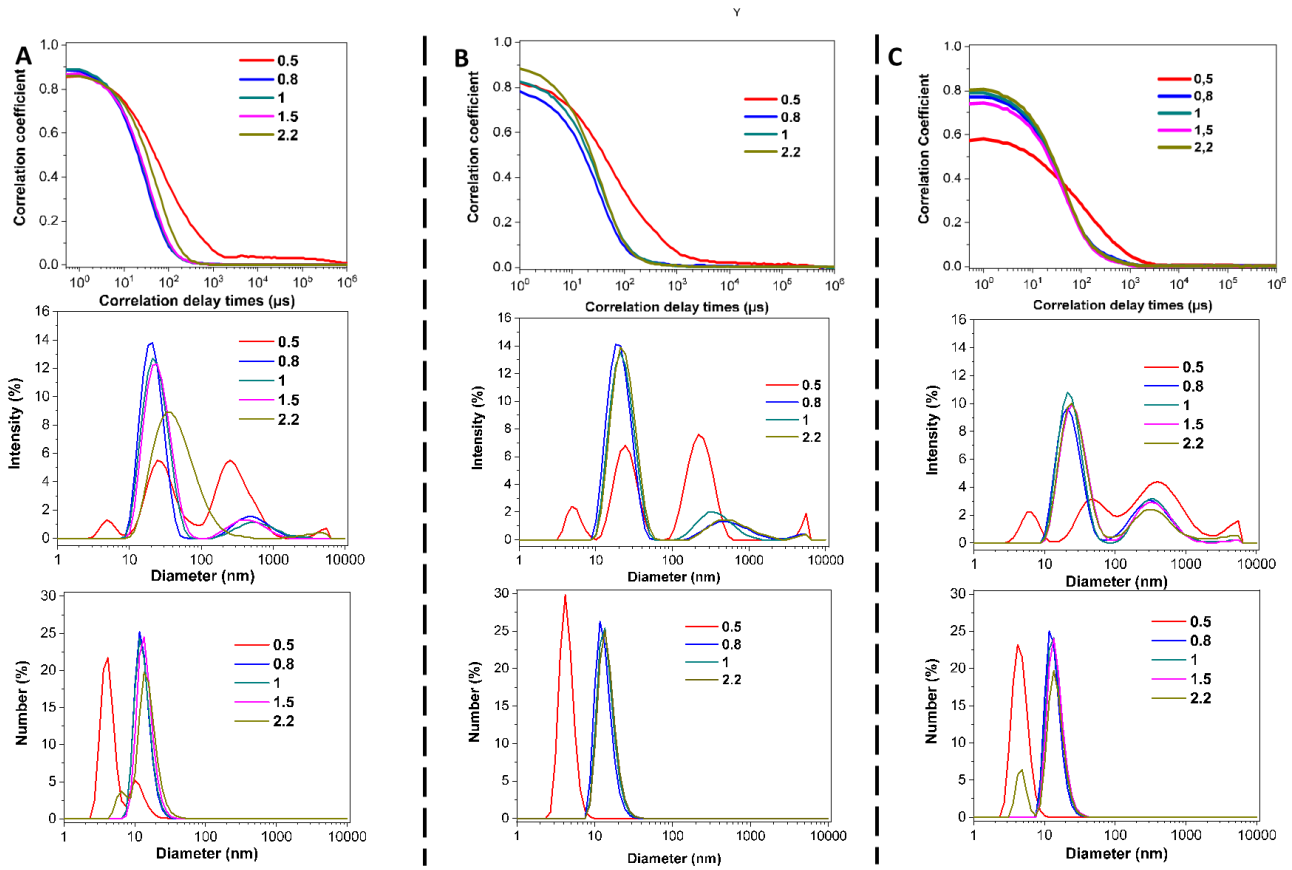


**Figure S5.** From top to bottom: correlation functions and corresponding distribution average size in intensity or in number (NNLS method) at different R ratios of: A) Gd<sup>3+</sup>/PAA<sub>32</sub>-*b*-PVP<sub>59</sub>, B) Y<sup>3+</sup>/PAA<sub>32</sub>-*b*-PVP<sub>59</sub> and C) Eu<sup>3+</sup>/PAA<sub>32</sub>-*b*-PVP<sub>59</sub>.

## Multi-angle dynamic light scattering experiments

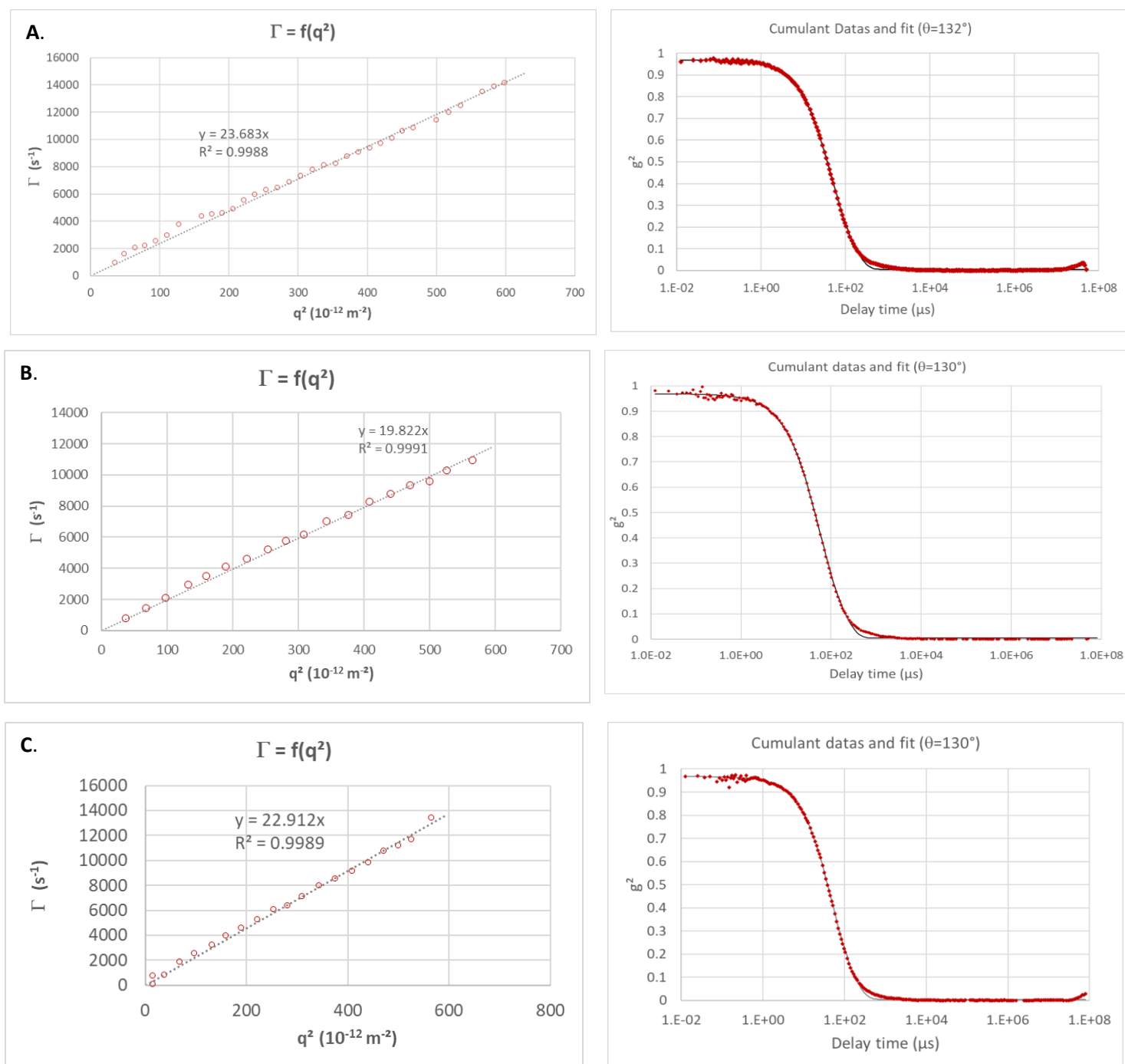


**Figure S6.** Analysis of multi-angle DLS data: A)  $\text{Gd}^{3+}/\text{PAA}_{32}\text{-}b\text{-PVP}_{59}$ , B)  $\text{Y}^{3+}/\text{PAA}_{32}\text{-}b\text{-PVP}_{59}$  and C)  $\text{Eu}^{3+}/\text{PAA}_{32}\text{-}b\text{-PVP}_{59}$  HPICs ( $R=1$ ). Left: Decay rate  $\Gamma$  versus the scattering vector  $q$  using the cumulant method. Right: Typical  $g_2$  correlogram (red circles) obtained for a defined angle. In black, best fit using the cumulant method with the M-STORMS software.<sup>[64]</sup>

Zeta potential

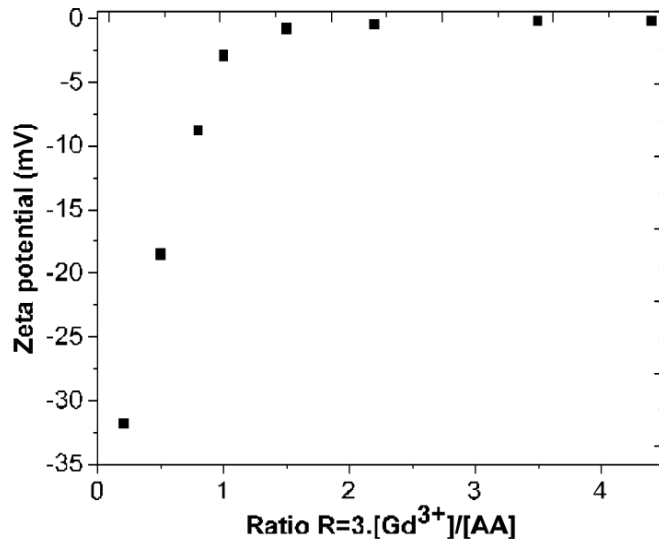


**Figure S7.** Evolution of zeta potential from Gd<sup>3+</sup>/PAA<sub>32</sub>-*b*-PVP<sub>59</sub> mixtures versus the R ratio.

2.2. Transmission electron microscopy (TEM) and high-angle annular dark-field scanning transmission electron microscopy (HAADF-STEM) experiments.

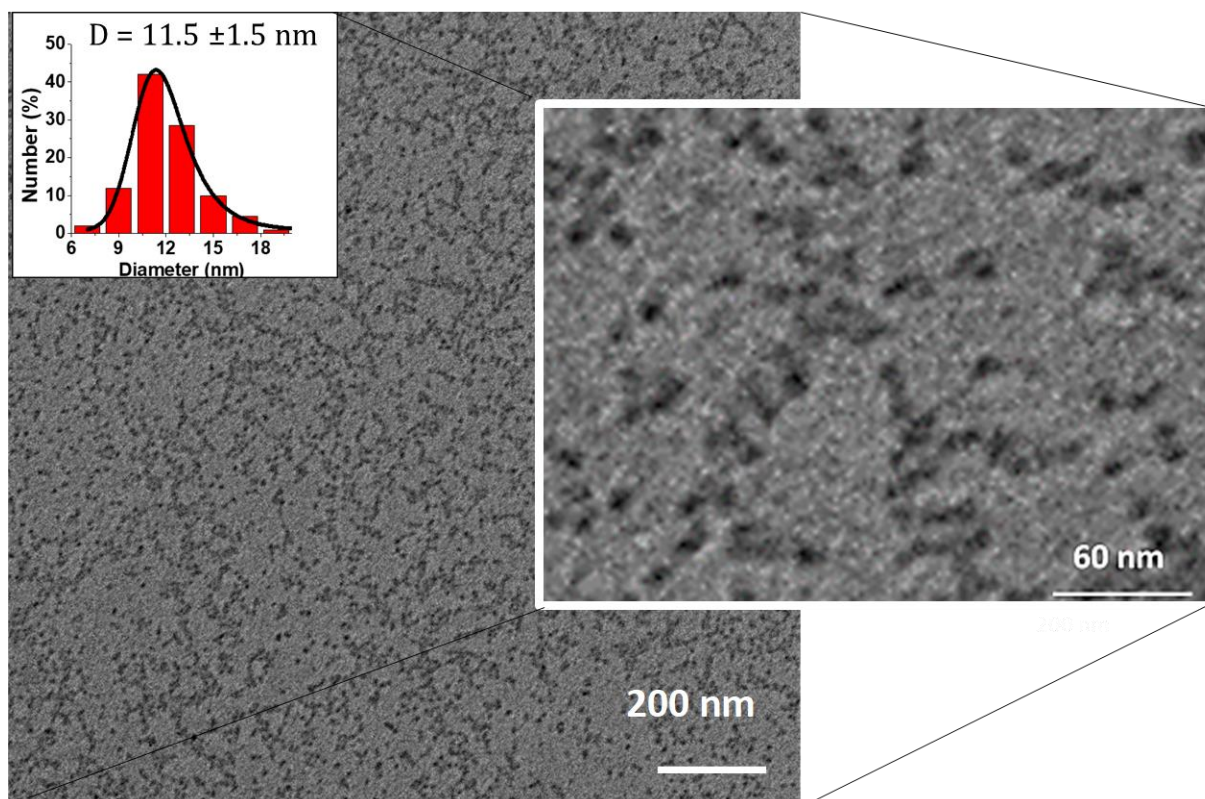
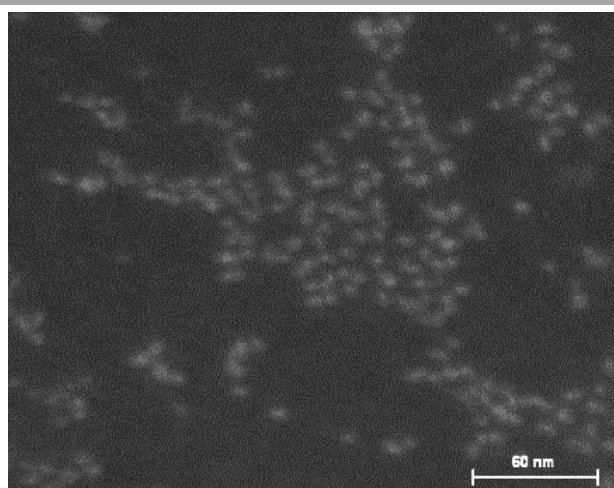
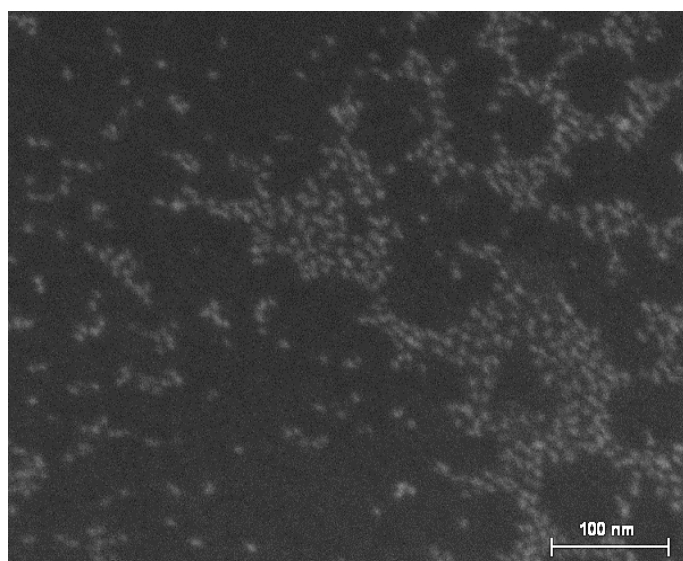
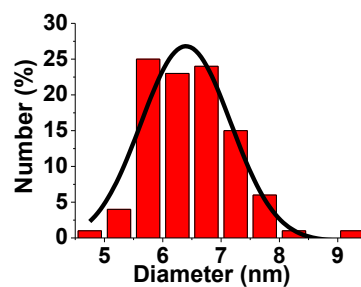


Figure S8A. Conventional TEM images of the Gd<sup>3+</sup>/PAA<sub>32</sub>-*b*-PVP<sub>59</sub> HPICs and the corresponding size histogram (R=1).



$d=6.4 \text{ nm}$  and  $\sigma=0.8 \text{ nm}$



**Figure S8B** STEM-HAADF images of the  $\text{Gd}^{3+}/\text{PAA}_{32}\text{-}b\text{-PVP}_{59}$  HPICs and the corresponding size histogram ( $R=1$ ).

**NB:** Attempts to provide STEM-EDS (elemental dispersive spectroscopy) elemental mapping of  $\text{Gd}(K\alpha)$  failed due to the weak signal provided by the scanned region, confirming the low density of gadolinium ions in the core of the Gd-polymer nanoparticles

### 2.3. Photophysical Experiments

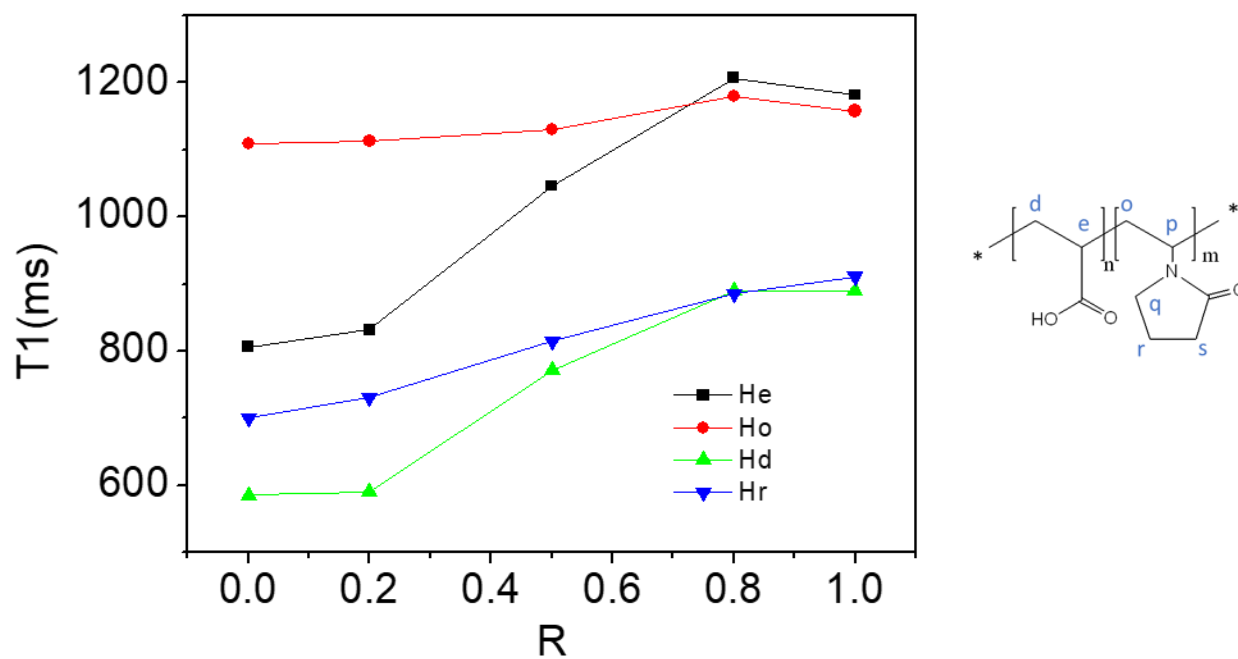
Lifetimes  $\tau$  (uncertainty  $\leq 5\%$ ) were determined by monitoring the decay at 615 nm, following pulsed excitation. The luminescence decay curves were fitted by an equation of the form  $I(t) = I(0) \exp(-t/\tau)$  by using Origin curve-fitting program, where  $I(t)$  is the total luminescence intensity at time  $t$ ,  $I(0)$  the luminescence intensity at  $t=0$ ms, and  $\tau$  is the corresponding lifetime.

R	$\tau_{\text{H}_2\text{O}}$ (ms)	$\tau_{\text{D}_2\text{O}}$ (ms)	Water molecules
0.2	0.24	2.77	3.9
0.5	0.26	2.65	3.5
0.8	0.24	2.51	3.8
1.0	0.25	2.37	3.6

**Table S1.** Lifetimes in  $\text{H}_2\text{O}$  ( $\tau_{\text{H}_2\text{O}}$ ) and in  $\text{D}_2\text{O}$  ( $\tau_{\text{D}_2\text{O}}$ ) for each R ratio ( $R=3.[\text{Eu}^{3+}]/[\text{AA}]$ ) and the corresponding number of water molecules ( $q$ ) in the first coordination sphere of europium ion calculated with Equation 1 from Supkowski et al.<sup>1</sup>

$$\text{Equation 1 : } q = 1.11 * (1/\tau_{\text{H}_2\text{O}} - 1/\tau_{\text{D}_2\text{O}} - 0,31)$$



2.5.  $^1\text{H}$  NMR experiments- $\text{Y}^{3+}$ -titration

**Figure S10.** Longitudinal relaxation time ( $T_1$ ) registered for the protons corresponding to the (PAA) block (Hd and He) and to the (PVP) block respectively (Ho and Hr) as a function of R ratio.

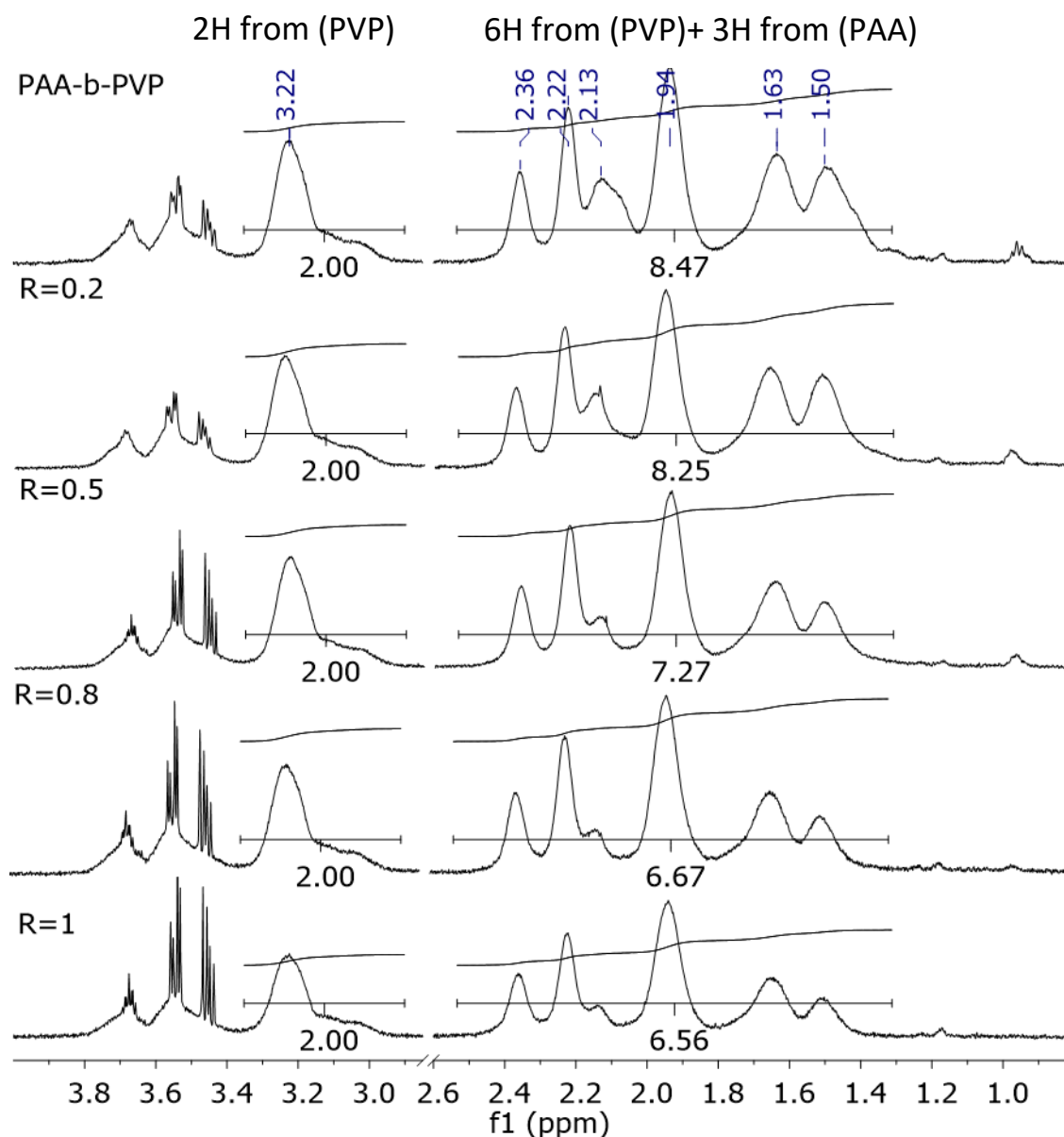


**Figure S11.**  $^1\text{H}$  NMR (600MHz) spectra (in 10% vol.  $\text{D}_2\text{O}$  and 90% vol.  $\text{H}_2\text{O}$  298 K) of  $\text{Y}^{3+}/\text{PAA}_{32}\text{-}b\text{-PVP}_{59}$  HPICs for  $R=0, 0.2, 0.5, 0.8$  and  $1$  ([polymer] = 0.1% wt., impurities at 3.5 ppm belong to dioxane derivative species, used as solvent)

In order to calculate the evolution of the integral ratio of the protons associated to the carboxylate block to the ones of the PVP block (PAA/PVP ratio), with the ratio  $R$  ( $R=3 \cdot [\text{Y}^{3+}]/[\text{AA}]$ ), the signals of the protons of the PAA and PVP between 1.2 and 2.6 ppm were integrated together and normalized to the signal of the PVP protons at 3.22 ppm. This strategy was adopted due to the superposition of the signal of the PAA with the one of the PVP in the region 1.2-2.6ppm.(Figure 4F in the publication)

## Calculation example for R=1:

$$6H(\text{PVP})+3H(\text{PAA})=6.56$$

$$2H(\text{PVP})=2 \Rightarrow 1H(\text{PVP})=1$$

$$\Rightarrow 3H(\text{PAA})=0.56 \Rightarrow 1H(\text{PAA})=0.56/3 \Rightarrow \text{PAA/PVP ratio} = 0.56/3 = 0.18$$

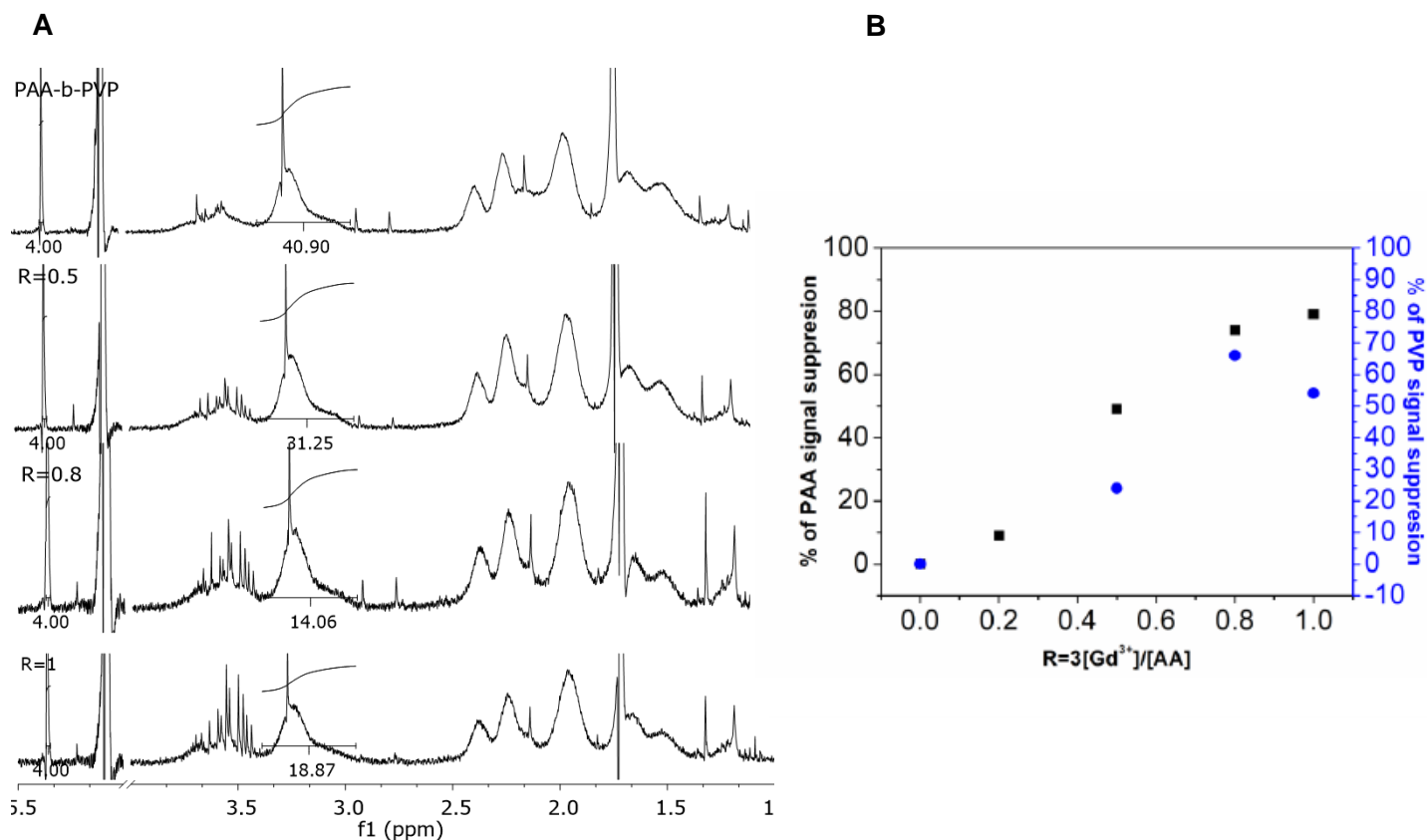


**Figure S12.** A)  $^1\text{H}$  NMR (300MHz) spectra (in 10% vol.  $\text{D}_2\text{O}$  and 90% vol.  $\text{H}_2\text{O}$  298 K) of  $\text{Y}^{3+}/\text{PAA}_{32}\text{-}b\text{-PVP}_{59}$  HPICs for  $R = 0, 0.5, 0.8$  and  $1$  ([polymer] = 0.1% wt.) evidencing the decrease of the signal intensity of the PVP block compared to that of the trioxane as internal standard (5.4 ppm). The trioxane was present in a constant concentration in  $\text{CDCl}_3$  in a capillary introduced in the NMR tube. Additional residual solvent peak were present at 1.7, 2.1 and 3.5 ppm. B) Percentage of the PAA and PVP block signal suppression as a function of R ratio.

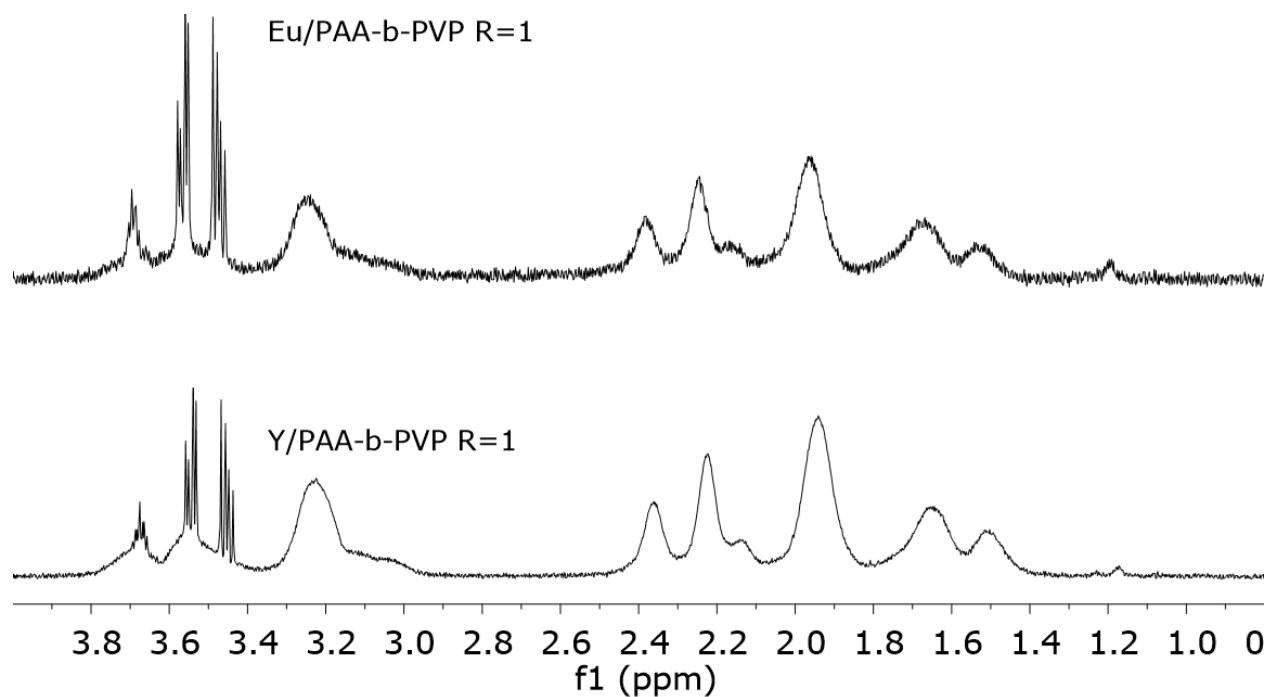


**Figure S13.**  $^1\text{H}$  NMR spectra ((in 10% vol.  $\text{D}_2\text{O}$  and 90% vol.  $\text{H}_2\text{O}$  298 K)) of  $\text{Eu}^{3+}/\text{PAA}_{32}\text{-}b\text{-PVP}_{59}$  and  $\text{Y}^{3+}/\text{PAA}_{32}\text{-}b\text{-PVP}_{59}$  HPICs for R= 1 ([polymer]=0.1% wt.)

## 2.6. Random vs. block copolymer for the formation of HPICs

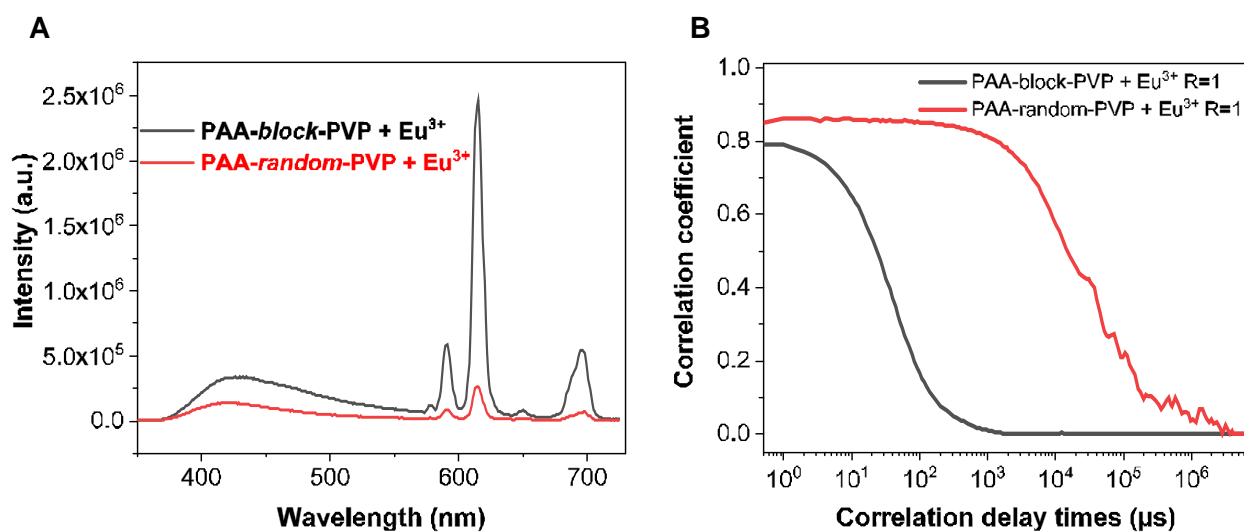


**Figure S14.** A) Commercial random PAA<sub>416</sub>-*r*-PVP<sub>270</sub> copolymer vs. block PAA<sub>32</sub>-*b*-PVP<sub>59</sub> copolymer: comparison of emission spectra ( $\lambda_{\text{ex}}=325$  nm) and B) DLS correlograms of Eu<sup>3+</sup>/PAA<sub>32</sub>-*b*-PVP<sub>59</sub> HPICs and Eu<sup>3+</sup>/PAA<sub>416</sub>-*r*-PVP<sub>270</sub> mixture ([polymer]=0.2% wt) for R=1.

### 3. Colloidal stability of HPICs and properties in biological medium

#### 3.1. Stability in the presence of different concentrations of NaCl

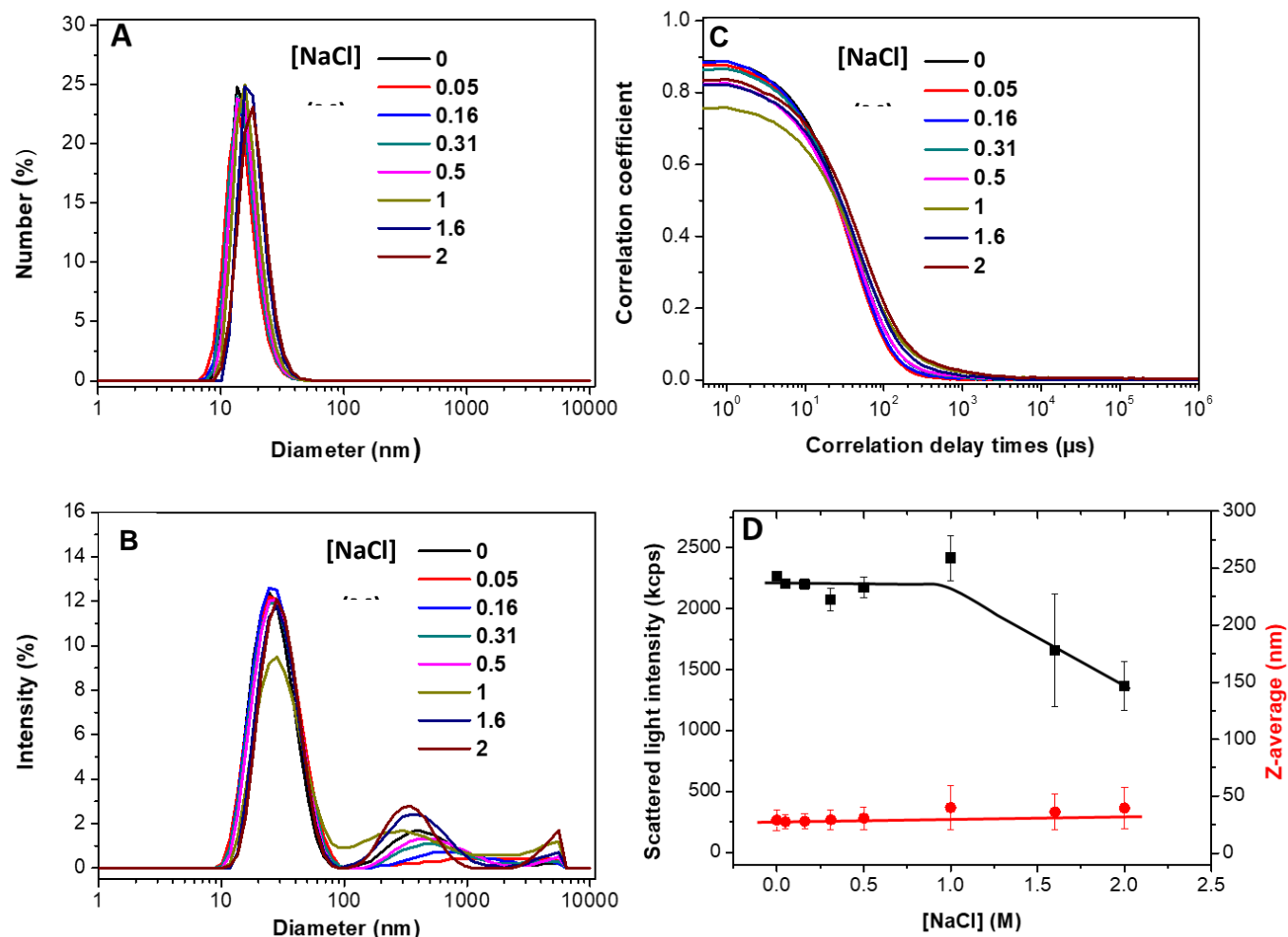


**Figure S15.** Colloidal stability of  $\text{Gd}^{3+}/\text{PAA}_{32}\text{-}b\text{-PVP}_{59}$  HPICs for  $R=1$  as determined by mono-angle DLS measurements. A) Number-averaged and B) intensity-averaged size distributions of hydrodynamic diameter of HPICs obtained from the analysis of correlograms (C) at different concentrations of NaCl. D) Z-average size (diameter in nm, in red) with corresponding scattered light intensity (in black) as a function of NaCl concentration. The lines are just guide for the eyes.

## 3.2. Influence of pH

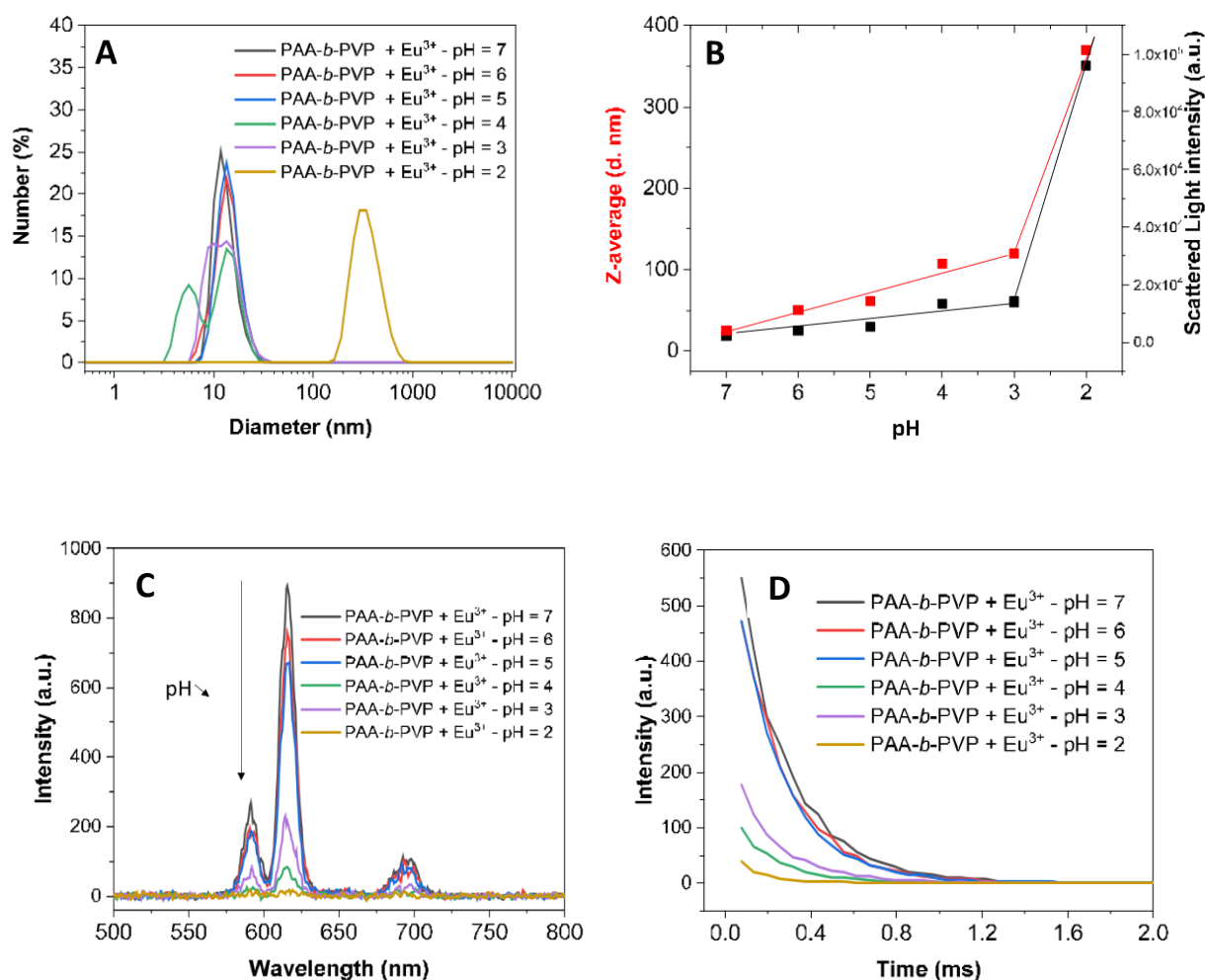
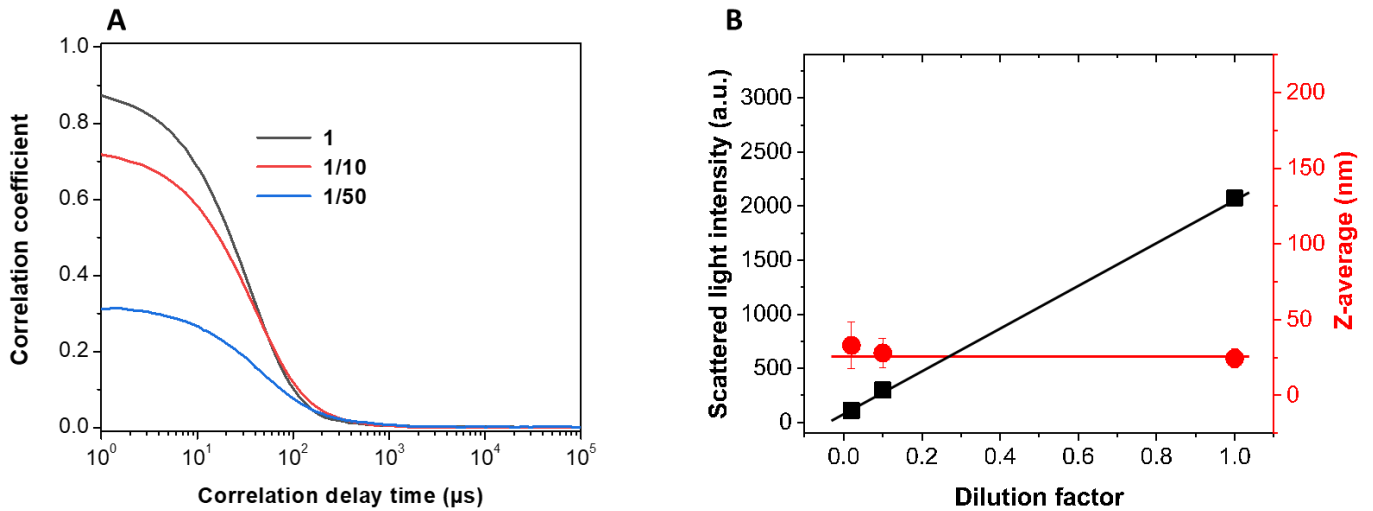


**Figure S16.** Colloidal stability of Eu<sup>3+</sup>/PAA<sub>32</sub>-b-PVP<sub>59</sub> HPICs for R=1 as a function of pH. A) Number-averaged size distribution of hydrodynamic diameter measured by mono angle DLS. B) Typical evolutions of the scattered light intensity (black squares) and Z-average diameter (red squares) obtained from the analysis of correlogram. C) Emission spectra of Eu<sup>3+</sup>/PAA<sub>32</sub>-b-PVP<sub>59</sub> HPICs (an unexplained tendency was observed at pH =3 and 4). D). Lifetimes measurements. [PAA-*b*-PVP] = 0.1%wt in water, [Eu<sup>3+</sup>] = 1.3 mM.

pH	Lifetime in H <sub>2</sub> O (ms)	Lifetime in D <sub>2</sub> O (ms)	Number of water molecules <i>q</i>
7	0.23	2.23	3.9
6	0.23	1.96	3.9
5	0.22	1.75	4.1
4	0.19	0.92	4.2
3	0.20	1.06	4.3
2	0.12	0.58	7.1

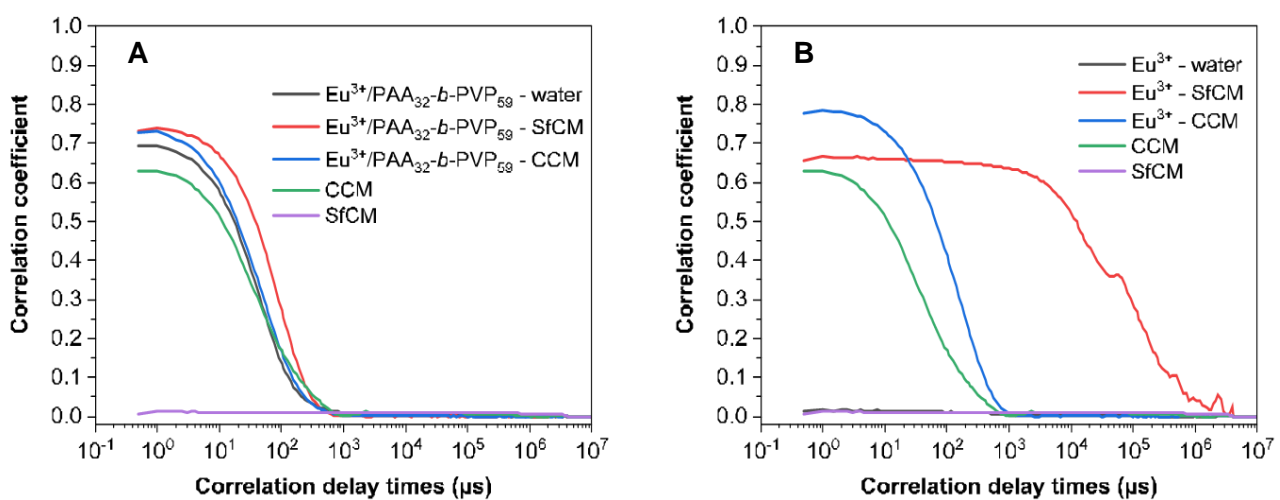
**Table S2.** Lifetimes in H<sub>2</sub>O ( $\tau_{H_2O}$ ) and in D<sub>2</sub>O ( $\tau_{D_2O}$ ) and the corresponding number of water molecules (*q*) in the first coordination sphere of europium ion calculated with Equation 1 from Supkowski et al.<sup>1</sup>

### 3.3. Stability as a function of the dilution factor



**Figure S17** : A) Evolution of the correlogram obtained for various dilution factor of a  $Gd^{3+}/PAA_{32}\text{-}b\text{-}PVP_{59}$  HPICs sample ( $R=1$ ) (scattering angle:  $173^\circ$ , mono-angle DLS instrument). It could be observed that the correlogram is not shifted towards longer correlation delay times, indicating that no larger nanostructures were obtained by diluting the sample. The correlation coefficient decreases in intensity because of the decrease of the recorded signal. B) Evidence of the constant mean diameter, Z-average value with dilution and decrease of the scattered light intensity.

### 3.4. Stability in complete cell culture medium



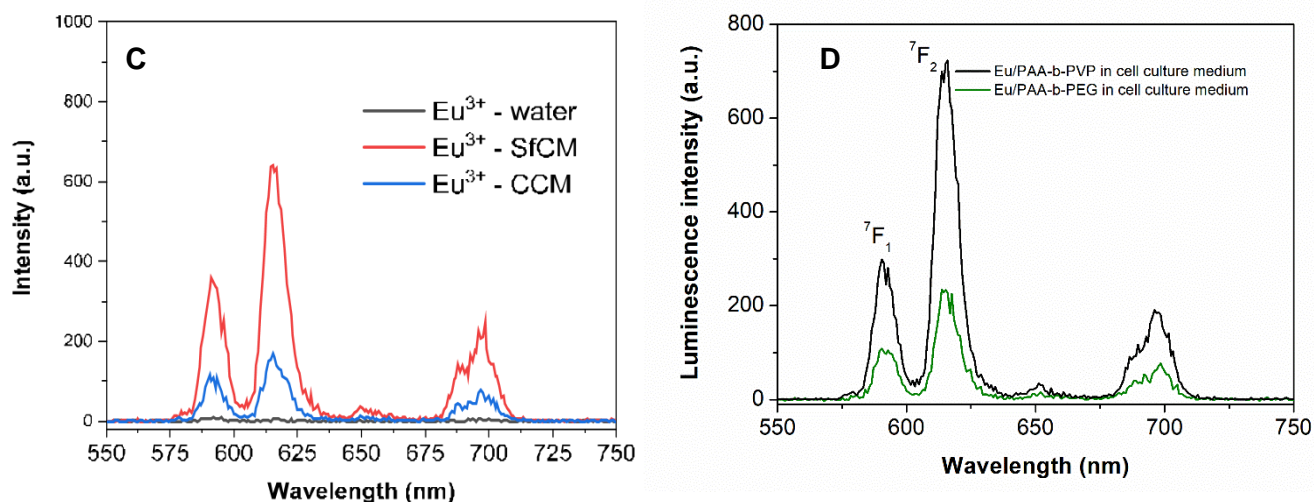


**Figure S18** : A) DLS measurements (correlation functions) of Eu<sup>3+</sup>/PAA<sub>32</sub>-b-PVP<sub>59</sub> HPICs (R=1) in water, serum-free culture medium (SfCM) and complete cell culture medium (CCM), respectively and of the SfCM and CCM alone. B) DLS measurements (correlation functions) of Eu<sup>3+</sup> free ions in water, SfCM and CCM. C) Time-resolved emission spectra ( $\lambda_{\text{ex}}=256$  nm) of Eu(NO<sub>3</sub>)<sub>3</sub> in water, SfCM and CCM. D) Eu<sup>3+</sup>/PAA<sub>32</sub>-b-PVP<sub>59</sub> HPICs (R=1) and of Eu<sup>3+</sup>/PAA<sub>3k</sub>-b-PEG<sub>6k</sub> HPICs (R=1) in CCM at the same concentration.

#### 4. Relaxivity measurements

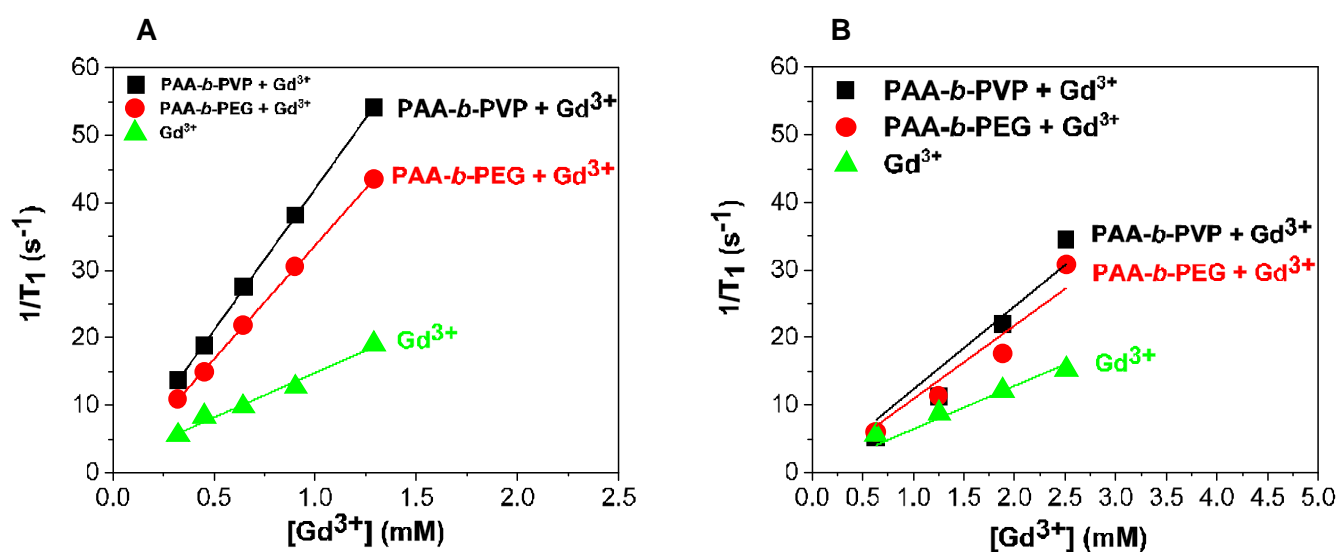


**Figure S19** : Change in the longitudinal relaxation time as a function of the concentration of A) Gd<sup>3+</sup> ions in water and B) in complete cell culture medium.

#### 5. References

[1] R. M. Supkowski and W. DeW. Horrocks, *Inorg. Chim. Acta*, **2002**, 340, 44.